

High Rayleigh number convection with double diffusive fingersE. Hage¹ and A. Tilgner¹*Institute of Geophysics, University of Göttingen, Friedrich-Hund-Platz 1,
37077 Göttingen, Germany*

(Dated: 4 January 2018)

An electrodeposition cell is used to sustain a destabilizing concentration difference of copper ions in aqueous solution between the top and bottom boundaries of the cell. The resulting convecting motion is analogous to Rayleigh-Bénard convection at high Prandtl numbers. In addition, a stabilizing temperature gradient is imposed across the cell. Even for thermal buoyancy two orders of magnitude smaller than chemical buoyancy, the presence of the weak stabilizing gradient has a profound effect on the convection pattern. Double diffusive fingers appear in all cases. The size of these fingers and the flow velocities are independent of the height of the cell, but they depend on the ion concentration difference between top and bottom boundaries as well as on the imposed temperature gradient. The scaling of the mass transport is compatible with previous results on double diffusive convection.

I. INTRODUCTION

Double diffusive convection occurs in a fluid whose density depends on two properties with different diffusion constants. The prototypical example is water whose density depends on temperature and salt concentration. This particular combination is relevant in oceanography and the interest in double diffusive convection historically originated in this field. More applications have since emerged in geophysics, astrophysics, and engineering¹. Double diffusive convection differs from ordinary Rayleigh-Bénard convection in that two fundamentally new flow structures can appear: Layers and fingers. Fingers are vertically oriented long and narrow regions of up- or downwelling fluid which can occur if the fluid property with the large diffusion coefficient (for example temperature) imposes a stabilizing gradient on the fluid, whereas the property with the small diffusion constant (the salt concentration in the oceanographic example) is unstably stratified. The basic principles of finger formation are well understood since linear stability analysis already predicts convection with fingers². Layers dividing the fluid volume into several sections in the vertical direction with little advective transport between the layers is frequently observed in double diffusive systems, irrespective of which component is stabilizing and which is destabilizing. The necessary conditions for layer formation remain controversial³⁻⁵.

The experiments reported here deal with a double diffusive convective system which forms fingers but no layers so that various scaling laws obeyed in the finger regime can be determined accurately.

A popular experimental setup for the study of double diffusive convection has been water with gradients of salt and sugar concentrations. The diffusion coefficients of salt and sugar differ by a factor of about 3. However, the ratio of the diffusivities of temperature and salt is much larger, typically around 100. The large aspect ratio of fingers makes their numerical simulation difficult. Experiments on the other hand have a problem in maintaining a steady state. Many experiments start from an initial distribution of salt and temperature and let the salt stratification disappear in the course of time. Some results may then depend on whether an experiment was started from a continuous stratification or a step function in the salt distribution⁶. One is therefore interested in experiments capable of keeping both constant temperature and concentration differences between top and bottom boundaries. Maintaining a temperature difference is simple, but the salt stratification is problematic. One

solution is to use an apparatus with permeable membranes as top and bottom boundaries^{7,8}. Water tanks with constant temperature and salt concentration placed outside the convecting volume on the other side of each membrane guarantee steady conditions in the experimental cell.

An alternative solution to the problem consists in using an electrochemical system. Convection in electrochemical cells with vertical electrodes has been studied at least since 1949^{9,10}. Even an application to double diffusion with horizontal gradients appeared¹¹. Electrochemical convection was later noted in a cell with horizontal electrodes¹² and developed into an analogy for Rayleigh-Bénard convection¹³. The principle of the system used most frequently and also in this paper is to fill a cell with a solution of $CuSO_4$ and to place copper electrodes at the top and bottom of the cell. When an electric current is sent through the cell, copper dissolves from one electrode and is deposited on the other electrode. A non-uniform spatial distribution of copper ion concentration is responsible for buoyancy and convection. In order for copper ions to behave in the same way as salt or temperature in a Rayleigh-Bénard experiment, one needs to make sure that the ions diffuse and are advected, but do not experience a force in the electrical field due to the potential difference applied between the two electrodes. This is achieved by dissolving a large concentration of another electrolyte such as H_2SO_4 which does not participate in the chemical reaction at the electrodes and which screens the electrical field in the bulk of the cell. The electrical field separates ions of the electrolyte which accumulate in charged layers of microscopic thickness next to each electrode so that the copper ions move essentially in a field free environment. Refs. 13 and 14 provide more details about the electrochemical system and its relation to Rayleigh-Bénard convection.

In the experiments presented here, the two copper electrodes are regulated in temperature, with a cold cathode at the bottom and a warm anode at the top. Temperature is thus stabilizing and the ion concentration is destabilizing. Mass transport is conveniently measured in this system because it is directly related to the current flowing through the electrodes. Since the working fluid is transparent, we also use particle image velocimetry (PIV) to measure velocity and finger sizes. We are able to vary the chemical and thermal Rayleigh numbers over several orders of magnitude. It will be shown below that the thermal stratification is important for the mass transport and leads to fingers even if the thermal Rayleigh number is much smaller than the chemical one. The main results will be finger

widths, flow velocities and mass transport in convection with double diffusive fingers in a statistically steady state.

The next section presents the experimental apparatus and methods. The results are summarized in table I and discussed in the third section.

II. EXPERIMENTAL PROCEDURES

This section will describe a novel experimental realization of a double diffusive convection cell in which temperature and ion concentration are the two diffusers. It is useful to first introduce some nomenclature and definitions to describe the system. Double diffusive systems are characterized by four control parameters: There are two diffusivity ratios, the Prandtl number Pr and the Schmidt number Sc ,

$$Pr = \frac{\nu}{\kappa} \quad , \quad Sc = \frac{\nu}{D} \quad (1)$$

in which ν stands for the kinematic viscosity of the convecting fluid, κ for its thermal diffusivity, and D for the ion diffusion constant. There are furthermore the thermal and chemical Rayleigh numbers, Ra_T and Ra_c ,

$$Ra_T = \frac{g\alpha\Delta TL^3}{\kappa\nu} \quad , \quad Ra_c = \frac{g\beta\Delta cL^3}{D\nu} \quad (2)$$

with g the gravitational acceleration and L the cell height. The two expansion coefficients α and β determine variations of density ρ around a reference state with density, temperature, concentration and pressure ρ_0 , T_0 , c_0 and p_0 via

$$\alpha = -\frac{1}{\rho_0} \left(\frac{\partial \rho}{\partial T} \right)_{c_0, \rho_0, p_0} \quad , \quad \beta = \frac{1}{\rho_0} \left(\frac{\partial \rho}{\partial c} \right)_{T_0, \rho_0, p_0} \quad (3)$$

Both α and β are positive. The sign convention for the Rayleigh numbers used in this paper is such that negative Rayleigh numbers indicate a stable stratification. This implies that

$$\Delta T = T_{\text{bottom}} - T_{\text{top}} \quad , \quad \Delta c = c_{\text{top}} - c_{\text{bottom}} \quad (4)$$

with the subscripts indicating the boundary at which temperature T or concentration c are evaluated. Another dimensionless number in common use which will become useful below is the density ratio Λ :

$$\Lambda = \frac{Ra_T}{Ra_c} \frac{\kappa}{D} = \frac{\alpha\Delta T}{\beta\Delta c} \quad (5)$$

Λ quantifies the ratio of thermal and chemical buoyancy forces.

The electrochemical aspects of the experiment are essentially the same as in ref. 13. The cell was made of two copper electrodes of 1cm thickness painted with varnish on all surfaces which were not in contact with the electrolyte. Water from thermostats was circulated through pipes welded onto the copper plates in order to regulate their temperature. The sidewalls were made of four plexiglass plates 1cm thick epoxied together to form a rectangular frame. Four of these frames have been used, all with a cross section of $20\text{cm} \times 20\text{cm}$ and heights of $L = 2\text{cm}, 4\text{cm}, 8\text{cm}$ and 20cm .

The cell was filled with a solution of CuSO_4 in 1 molar sulfuric acid. The solution was prepared by dissolving $\text{CuSO}_4 \cdot (\text{H}_2\text{O})_5$ at a few tens of mmol/l . In between measurements, samples of the solution were extracted from the cell in order to check with optical absorption spectroscopy that the copper concentration remained constant. For PIV measurements, polyamide particles $100\mu\text{m}$ in diameter were added to the solution. The material constants necessary for the determination of Pr , Sc , Ra_T and Ra_c were taken from ref. 14.

The concentration difference Δc is not directly under control in these experiments. It is known only for suitable settings of the electrolytic cell. If no current flows through the cell, $\Delta c = 0$ and the concentration is everywhere equal to the average concentration c_0 . At small voltages applied to the electrodes, the current rises for increasing voltage. Only diffusion transports the copper ions close to the boundaries so that a concentration gradient must exist near each electrode. The copper ions are depleted near the cathode and their concentration is increased near the anode. The so called limiting current is reached when the copper ion concentration at the cathode is down to zero¹⁵. It is concluded from symmetry that the anode concentration is then $2 \cdot c_0$, and therefore the concentration difference across the cell is $\Delta c = 2 \cdot c_0$. Increasing the voltage further cannot increase the current any more and a plateau is reached in the characteristic curve of current versus voltage. An increase beyond the limiting current is only possible for voltages large enough to allow another chemical reaction, such as water dissociation.

The voltage range for which the limiting current is obtained depends on the cell height, the concentration c_0 , and ΔT . Preliminary measurements of the voltage characteristic for $\Delta T = -4\text{K}$ and $\Delta T = 0$ were performed for all heights and concentrations in order to determine the appropriate voltage used later to create and maintain the concentration difference of $\Delta c = 2 \cdot c_0$.

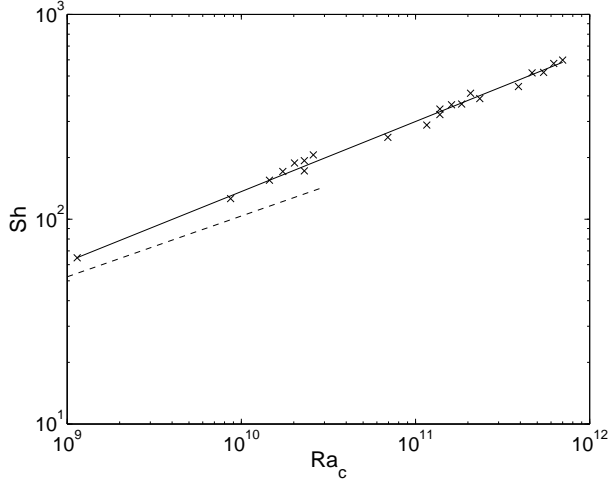


FIG. 1. Sh as a function of Ra_c in a fluid with uniform temperature. The dashed line indicates $Sh = 0.14Sc^{-0.03}Ra_c^{0.297}$, which is the functional dependence proposed in 16. The continuous line is given by $Sh = 0.052Ra_c^{0.34}$.

The Sherwood number, which is the same thing as the chemical Nusselt number, is directly proportional to the number of ions transported from top to bottom divided by the purely diffusive current, so that the Sherwood number can be determined by

$$Sh = \frac{jL}{zFD\Delta c} \quad (6)$$

if j is the current density, z the valence of the ion ($z = 2$ for Cu^{2+}) and F Faraday's constant. A transference number, which must sometimes be taken into account when computing Sherwood numbers¹³ is so small in the present case that it was neglected.

The double diffusion experiment was preceded by another experiment in which the $CuSO_4$ solution was kept isothermal in cubes of side length $5cm$, $10cm$ and $15cm$. The dependence of Sh on Ra_c obtained from this preliminary experiment is shown in fig. 1. This figure contains also one point at $Ra_c \approx 10^9$ obtained in one of the cells later used for the double diffusive experiments (the one of height $2cm$). These results should be identical to measurements of the Nusselt number in a thermal convection experiment. Figure 1 also shows the $Sh(Ra_c)$ dependence extrapolated from measurements in ref. 16, performed in a cylindrical cell at Rayleigh numbers between 2×10^7 and 3×10^{10} and Prandtl numbers between 4.3 and 1350. In the interval of Rayleigh numbers where both experiments overlap, there is a discrepancy of about 20%. This may be due to the different cell geometries, but discrepancies of this order of magnitude are not unusual when comparing different Rayleigh-

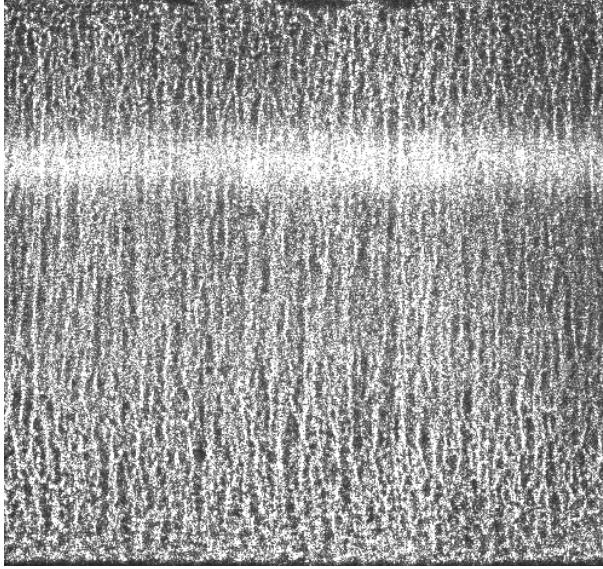


FIG. 2. Shadowgraph picture taken across the cell of height 80mm 15min after the voltage was switched on for $Ra_c = 1.15 \times 10^{11}$ and $Ra_T = -9.70 \times 10^7$. The bright horizontal bar is an artefact of the illumination. The picture covers the entire height of the cell and a width of 85mm .

Bénard experiments at these Rayleigh numbers¹⁷.

A typical experimental run of double diffusion convection was performed as follows: Care was taken when filling the container that no air was trapped inside the cell. Then the top and bottom plates were set to the desired temperatures and enough time was allowed for a linear temperature gradient to establish. The voltage was then applied instantaneously and the current observed. During transients lasting from a few minutes to one hour, the current oscillated with decreasing amplitude and period until the limiting current was reached. After that time, the current fluctuated by less than 1% and a statistically stationary finger pattern filled the whole cell. This pattern could be observed in shadowgraph pictures taken in parallel, an example of which is shown in figure 2. The precise nature of the initial conditions turned out to be irrelevant for the final state. A few runs were started from uniform temperature and copper concentration, and the water circulation through the thermostats and the voltage were switched on simultaneously. This procedure led to longer transients but did not change the measurements thereafter.

PIV measurements were performed in the stationary state. The light beam of a 50mJ Nd:YAG laser system with two IR laser heads illuminated a vertical plane with a width of

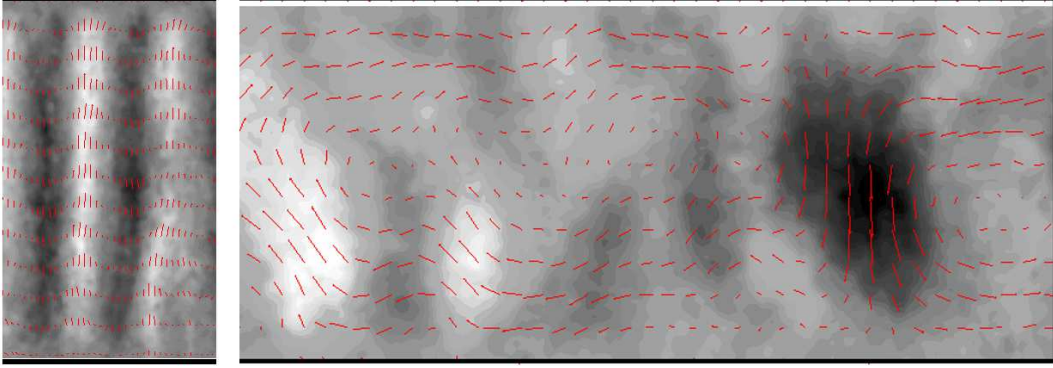


FIG. 3. Velocity field obtained from PIV measurements at $Ra_c = 1.05 \times 10^9$ and $Ra_T = -3.81 \times 10^5$ (left panel) and $Ra_c = 1.14 \times 10^9$ without any stabilizing temperature gradient (right panel). The picture shows the entire cell height of 20mm and extends over a width of 12mm (left) or 45mm (right). The lines (red online) indicate direction and velocity of the flow, the shade of gray depends on the vertical component of velocity which varies from -0.2mm/s to 0.2mm/s (left) and from -0.7mm/s to 0.7mm/s (right) in going from dark to bright. The left panel shows the average of 60 pictures taken during an interval of 15s in order to reduce the noise contained in any single PIV velocity field, and the right panel shows an average over 30 pictures.

approximately 3mm in the middle of the cell. The time separation between the two pulses varied between 50 and 1000ms depending on the Rayleigh numbers. A camera took pictures of an approximately square region extending from the top to the bottom electrode. An example of a velocity field deduced from PIV measurements is shown in figure 3. Once the fingers were established, they remained surprisingly steady, keeping their positions for 30min or longer. For each velocity field the *rms* velocity was calculated and averaged over all pictures to give the velocity V . From there, the non-dimensional measure of the velocity, the Reynolds number Re , is computed as

$$Re = \frac{VL}{\nu}. \quad (7)$$

For the determination of the finger size, the vertical velocities in the PIV velocity fields were Fourier transformed along the horizontal and the spectra averaged over all horizontal lines and all pictures. The location of the maximum of the spectrum yields the finger thickness. Independently, the finger thickness could simply be measured on the pictures with a ruler.

The accuracy of the determination of d is limited by the number of fingers visible on any one picture. The relative error on d is typically 10% . The error on V depends on the setting

of the PIV system and could be as large as 20 %. The limiting current is the most accurate of our measurements with an error of a few percent. There is also an uncertainty on the control parameters. The measurements at small ΔT suffer most from fluctuations in the temperature regulation. Moreover, the material constants are based on extrapolations from relatively few measurements¹⁴ which adds up to an uncertainty on the Rayleigh numbers on the order of 10 %.

L [cm]	$\frac{\Delta T}{L}$ [K/cm]	c_0 [mol/l]	Pr	Sc	Ra_T	Ra_c	$\frac{d}{L}$	Re	Sh
2.0	-10.00	0.025	8.8	2047.9	$-4.18 \cdot 10^6$	$+9.15 \cdot 10^8$	0.050	0.452	34.9
2.0	-10.00	0.030	8.9	2057.3	$-4.18 \cdot 10^6$	$+1.10 \cdot 10^9$	0.065	0.819	56.7
2.0	-10.00	0.034	9.3	2276.4	$-3.80 \cdot 10^6$	$+1.25 \cdot 10^9$	0.060	0.799	49.0
2.0	-10.00	0.044	8.9	2083.7	$-4.16 \cdot 10^6$	$+1.61 \cdot 10^9$	0.055	0.756	58.0
2.0	-10.00	0.055	9.0	2104.8	$-4.15 \cdot 10^6$	$+2.01 \cdot 10^9$	0.060	0.709	45.5
2.0	-5.00	0.015	8.8	2029.4	$-2.10 \cdot 10^6$	$+5.49 \cdot 10^8$	0.075	0.463	32.2
2.0	-5.00	0.023	8.8	2044.2	$-2.09 \cdot 10^6$	$+8.41 \cdot 10^8$	0.070	0.608	51.6
2.0	-5.00	0.031	8.9	2059.1	$-2.09 \cdot 10^6$	$+1.13 \cdot 10^9$	0.085	1.040	61.2
2.0	-5.00	0.037	9.3	2283.1	$-1.90 \cdot 10^6$	$+1.37 \cdot 10^9$	0.065	1.710	50.2
2.0	-5.00	0.044	8.9	2083.7	$-2.08 \cdot 10^6$	$+1.61 \cdot 10^9$	0.080	1.120	62.2
2.0	-5.00	0.052	9.0	2100.0	$-2.08 \cdot 10^6$	$+1.92 \cdot 10^9$	0.070	1.450	56.0
2.0	-3.00	0.015	8.8	2029.4	$-1.26 \cdot 10^6$	$+5.49 \cdot 10^8$	0.095	0.789	38.7
2.0	-3.00	0.026	8.8	2050.7	$-1.25 \cdot 10^6$	$+9.69 \cdot 10^8$	0.085	1.100	56.8
2.0	-3.00	0.033	8.9	2062.9	$-1.25 \cdot 10^6$	$+1.21 \cdot 10^9$	0.095	1.220	60.4
2.0	-3.00	0.044	8.9	2083.7	$-1.25 \cdot 10^6$	$+1.61 \cdot 10^9$	0.090	1.370	68.3
2.0	-3.00	0.050	9.4	2310.1	$-1.14 \cdot 10^6$	$+1.84 \cdot 10^9$	0.095	2.570	74.8
2.0	-1.00	0.016	8.8	2031.3	$-4.19 \cdot 10^5$	$+5.85 \cdot 10^8$	0.135	0.971	37.8
2.0	-1.00	0.024	8.8	2046.1	$-4.18 \cdot 10^5$	$+8.78 \cdot 10^8$	0.120	1.350	60.6
2.0	-1.00	0.029	9.3	2264.8	$-3.81 \cdot 10^5$	$+1.05 \cdot 10^9$	0.120	1.540	63.8
2.0	-1.00	0.032	9.3	2272.3	$-3.80 \cdot 10^5$	$+1.18 \cdot 10^9$	0.130	1.710	66.5
2.0	-1.00	0.033	8.9	2062.9	$-4.17 \cdot 10^5$	$+1.21 \cdot 10^9$	0.105	1.270	61.9
2.0	-1.00	0.042	8.9	2079.9	$-4.17 \cdot 10^5$	$+1.54 \cdot 10^9$	0.135	1.890	73.2
2.0	-1.00	0.048	9.4	2305.8	$-3.79 \cdot 10^5$	$+1.77 \cdot 10^9$	0.125	2.890	81.4
2.0	-0.50	0.030	9.1	2160.1	$-1.99 \cdot 10^5$	$+1.10 \cdot 10^9$	0.170	1.690	68.0
2.0	-0.25	0.031	8.9	2059.1	$-1.04 \cdot 10^5$	$+1.13 \cdot 10^9$	0.205	2.550	69.8
2.0	-0.10	0.030	9.3	2268.1	$-3.81 \cdot 10^4$	$+1.11 \cdot 10^9$	0.280	3.050	66.2
4.0	-3.00	0.013	9.2	2232.3	$-1.83 \cdot 10^7$	$+3.69 \cdot 10^9$	0.045	0.652	73.3
4.0	-3.00	0.049	9.4	2306.7	$-1.82 \cdot 10^7$	$+1.43 \cdot 10^{10}$	0.045	4.410	138.0
4.0	-2.00	0.014	9.2	2234.9	$-1.22 \cdot 10^7$	$+4.07 \cdot 10^9$	0.050	0.941	70.1
4.0	-2.00	0.050	9.4	2309.6	$-1.21 \cdot 10^7$	$+1.47 \cdot 10^{10}$	0.053	6.670	141.0
4.0	-1.00	0.011	9.2	2229.8	$-6.12 \cdot 10^6$	$+3.33 \cdot 10^9$	0.062	1.590	91.4
4.0	-1.00	0.048	10.4	2871.4	$-4.88 \cdot 10^6$	$+1.43 \cdot 10^{10}$	0.065	6.540	156.0
4.0	-0.50	0.011	9.2	2229.6	$-3.06 \cdot 10^6$	$+3.30 \cdot 10^9$	0.080	2.050	95.4
4.0	-0.50	0.050	9.4	2308.6	$-3.03 \cdot 10^6$	$+1.45 \cdot 10^{10}$	0.082	7.430	155.0
8.0	-1.00	0.011	10.3	2845.6	$-7.66 \cdot 10^7$	$+2.64 \cdot 10^{10}$	0.030	2.180	174.0
8.0	-1.00	0.049	9.4	2307.5	$-9.70 \cdot 10^7$	$+1.15 \cdot 10^{11}$	0.033	15.500	290.0
8.0	-0.75	0.011	9.2	2229.2	$-7.34 \cdot 10^7$	$+2.59 \cdot 10^{10}$	0.035	4.380	171.0
8.0	-0.75	0.050	10.4	2875.7	$-5.85 \cdot 10^7$	$+1.18 \cdot 10^{11}$	0.036	7.850	291.0
8.0	-0.50	0.049	10.4	2874.6	$-3.90 \cdot 10^7$	$+1.17 \cdot 10^{11}$	0.041	14.600	303.0
8.0	-0.25	0.011	10.3	2845.6	$-1.92 \cdot 10^7$	$+2.64 \cdot 10^{10}$	0.051	5.710	185.0
8.0	-0.25	0.049	9.4	2307.5	$-2.43 \cdot 10^7$	$+1.15 \cdot 10^{11}$	0.051	19.100	311.0
20.0	-0.50	0.031	8.9	2059.1	$-2.09 \cdot 10^9$	$+1.13 \cdot 10^{12}$	0.016	26.600	608.0
20.0	-0.10	0.030	8.9	2057.3	$-4.18 \cdot 10^8$	$+1.10 \cdot 10^{12}$	0.028	55.100	672.0

TABLE I. Summary of experimental results. The first three columns give the cell height, the applied temperature gradient, and the concentration of $CuSO_4$. The next four columns contain the nondimensional control parameters (Prandtl, Schmidt, thermal Rayleigh and chemical Rayleigh numbers) and the last three columns the nondimensional measured quantities (finger width, Reynolds and Sherwood numbers).

III. RESULTS AND DISCUSSION

The main quantitative results are contained in table I. The most important qualitative observation from shadowgraphs and PIV is that fingers exist at all. This is remarkable because apart from two exceptions, $|\Lambda| < 1$ in the experiments and the total density is unstably stratified so that fingers are not necessary for convection to start. One might also think that at $|\Lambda| = 10^{-2}$, the presence of the weak stable thermal stratification should be irrelevant for the chemical convection, but it is not. Fingers still appear. They are of course absent for $\Lambda = 0$. The isothermal experiments in figure 1 have $\Lambda = 0$ and it could be verified at the occasion of those preliminary experiments that a single convection roll forms in a cubic cell in this case and that the aspect ratio of convection rolls in the cell of height 20mm is compatible with what is known from ordinary Rayleigh-Bénard convection¹⁸.

Some more information about the structure of the fingers can be deduced from table I. The finger thickness always exceeds the concentration boundary layer thickness λ , which can be computed from the measured Sherwood number as

$$\lambda = \frac{L}{2Sh} \quad (8)$$

λ is small compared with the cell height L in all cases. Since the fingers extend across the entire height of the cell, they carry fluid directly from one boundary layer to the other. In a horizontal cross section, they must therefore consist of a core of size λ , which is the detached boundary layer, surrounded by the entraining fluid filling a cross section of size d . The ion exchange between neighboring fingers is small as long as the distance over which ions diffuse during the time it takes to transit from one boundary to the other is small compared with the finger size, i.e. as long as $(DL/V)^{1/2}/d = (Re Sc)^{-1/2}L/d \ll 1$. It can be seen from figure 4 that chemical exchange between fingers can be neglected for the experiments listed in table I, and that this will not be true any more around $|\Lambda| \approx 5$.

If there is no significant chemical diffusion across fingers, it is a simple matter to estimate Sh for $Sh \gg 1$ from the advective transport:

$$Sh \approx Sh - 1 = \frac{L}{D\Delta c} V \bar{c} \quad (9)$$

where \bar{c} denotes the concentration anomaly in a finger averaged over its cross section. $\bar{c} = \frac{1}{2}(\lambda/d)^2 \Delta c$ in a finger with circular or square cross section. This assumption is not compatible

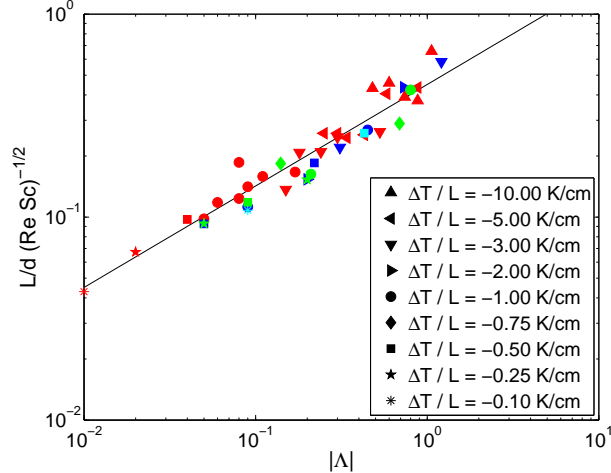


FIG. 4. $(Re Sc)^{-1/2}L/d$ as a function of $|\Lambda|$. The symbol shapes indicate the applied temperature gradient, the colors the height of the cell: 20mm (red), 40mm (dark blue), 80mm (green) and 200mm (light blue).

with the data in table I. If on the other hand fingers form sheets, $\bar{c} = \frac{1}{2}\lambda/d\Delta c$. Figure 5 shows that

$$Sh = \frac{1}{3}(Re Sc L/d)^{1/2} \quad (10)$$

is a good representation of the data from which we conclude that fingers have a lamellar shape.

Pr and Sc vary by less than 30% in table I so that a dependence on these parameters cannot be extracted from the data. It must be kept in mind that the prefactors in the power laws given below potentially depend on both Pr and Sc .

Let us now turn to the scaling of the finger width. Which parameters do we expect to determine this width? Long and narrow fingers should not be affected by far away boundaries. d should thus be independent of L . The fluid inside fingers carries the ion concentration from the boundary layer the finger started from. There are little diffusive losses during the transit, so that d should depend on Δc . Temperature on the other hand diffuses much more rapidly and fingers somewhere in the bulk do not know about the boundary temperatures. Temperature must enter the expression for d through the vertical gradient, $\Delta T/L$. A thickness d which depends on Δc and $\Delta T/L$ but is independent of L translates in nondimensional terms into a law of the form $d/L \propto |Ra_T|^{\gamma_1} Ra_c^{\gamma_2}$ with $4\gamma_1 + 3\gamma_2 = -1$. The scaling known from linear stability analysis, $d/L \propto |Ra_T|^{-1/4}$ belongs to this family of power

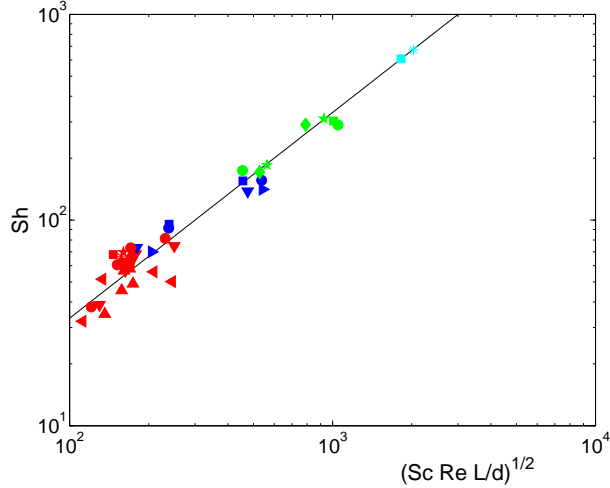


FIG. 5. Sh as a function of $Re Sc L/d$. The line is given by eq. (10). The symbols are the same as in figure 4.

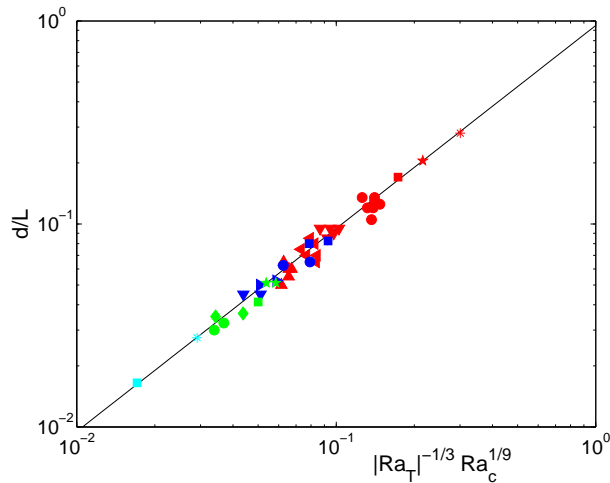


FIG. 6. d/L as a function of $|Ra_T|^{-1/3} Ra_c^{1/9}$. The line is given by eq. (11). The symbols are the same as in figure 4.

laws. However, the measured finger sizes in table I depend systematically on Ra_c . γ_1 and γ_2 have been determined from a linear regression applied to $\log(d/L) = A + \gamma_1 \log |Ra_T| + \gamma_2 \log Ra_c$. Our best fit obtained with that procedure yields $\gamma_1 = -0.32$ and $\gamma_2 = 0.086$, which is close to

$$\frac{d}{L} = 0.95 |Ra_T|^{-1/3} Ra_c^{1/9}. \quad (11)$$

The quality of this fit can be judged from figure 6. The important point is that the exponents obey $4\gamma_1 + 3\gamma_2 = -1$ so that eq. (11) is compatible with the general picture of fingers

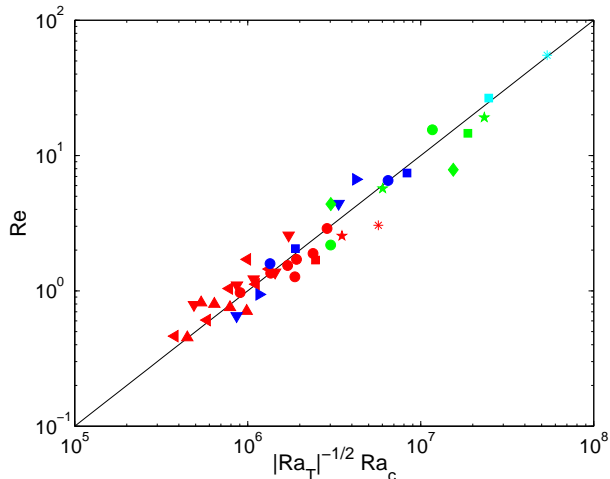


FIG. 7. Re as a function of $|Ra_T|^{-1/2} Ra_c$. The line is given by eq. (12). The symbols are the same as in figure 4.

delineated above.

The velocity should in the same fashion depend on Δc , $\Delta T/L$, but not on L . This means for the nondimensional variables that $Re \propto |Ra_T|^{\gamma_3} Ra_c^{\gamma_4}$ with $4\gamma_3 + 3\gamma_4 = 1$. An additional argument can be made concerning the dependence on the gravitational acceleration g . If buoyancy is balanced by viscous friction, one has to find $v \propto g$. However, a balance of linear terms is questionable because the linear terms all occur in linear stability analyses predicting fingers growing without bounds as a function of time. Saturation of finger velocity at finite amplitudes must involve the nonlinear terms, even if they are small. A balance between buoyancy and the advection term leads to $v \propto g^{1/2}$. A well known example of such a situation is Rayleigh-Bénard convection with a Rayleigh number near its critical value Ra_{crit} . The velocity near onset is small so that the Reynolds number is small, but experiments and weakly nonlinear analysis¹⁹ show that velocity is proportional to $(Ra - Ra_{\text{crit}})^{1/2} \propto g^{1/2}$. Returning to double diffusion, the additional requirement $v \propto g^{1/2}$ fully determines the exponents γ_3 and γ_4 to be $\gamma_3 = -1/2$ and $\gamma_4 = 1$. And indeed, a good fit to the data of table I is close to (see figure 7)

$$Re = 10^{-6} |Ra_T|^{-1/2} Ra_c \quad (12)$$

A linear regression applied to the logarithm of eq. (12) yields as best fit $Re = 2.9 \times 10^{-6} |Ra_T|^{-0.38} Ra_c^{0.87}$. However, Re is our measurement with the largest scatter and eq. (12) is only a marginally worse fit than the result of the linear regression. Another reason to

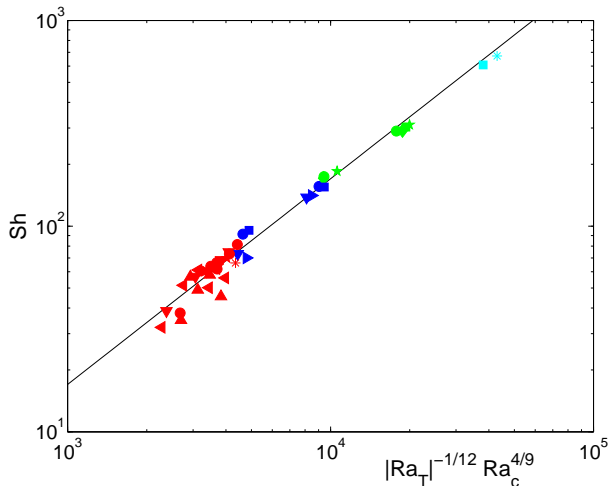


FIG. 8. Sh as a function of $|Ra_T|^{-1/12} Ra_c^{4/9}$. The line is given by eq. (13). The symbols are the same as in figure 4.

prefer eq. (12) over the direct fit is that eqs. (10, 11, 12) now fix the dependence of Sh on Ra_T and Ra_c to be

$$Sh = 0.016 |Ra_T|^{-1/12} Ra_c^{4/9} \quad (13)$$

which is shown in figure 8 and which is also recovered from a direct fit by linear regression to the logarithms, whose result is $Sh = 0.017 |Ra_T|^{-0.095} Ra_c^{0.45}$. Since $Sh \propto L/\lambda$ and since we may again argue that λ ought to depend on Δc , $\Delta T/L$ but not on L , we expect a scaling $Sh \propto |Ra_T|^{\gamma_5} Ra_c^{\gamma_6}$ with $4\gamma_5 + 3\gamma_6 = 1$. The exponents in eq. (13) obey this constraint.

According to eq. (13), the Sherwood number for finite $|Ra_T|$ should become larger than the Sherwood number for zero temperature stratification shown in figure 1 if Ra_c exceeds $|Ra_T|$ by five orders of magnitude. Such a combination of parameters has not been reached in the experiments. It is not a priori impossible that the Sherwood number for finger convection becomes larger than the Sherwood number for convection without fingers, but it seems more likely that the corresponding combinations of control parameters mark the limit of validity of eq. (13). Such a limit must exist somewhere because $Sh \rightarrow \infty$ for $|Ra_T| \rightarrow 0$ in eq. (13).

We finally compare the results of this section with previous work. The scalings of Sh , Re and d/L show that fingers in our experiments take the form of sheets. On the theoretical side, as analytic treatments of the planform selection problem became increasingly realistic, the predictions went from square cells to rolls and back to square cells^{20,21}. Experimentally, both square cells²² and cells in the form of rolls have already been observed²³.

Some experiments have determined a variation of finger widths with $|Ra_T|$ compatible with $|Ra_T|^{-1/4}$ ^{22,24}. This is the size of the fastest growing instability in a fluid layer with uniform temperature and salt gradients. Starting from a step change in temperature and salinity, ref. 6 found numerically a finger width scaling as $|Ra_T|^{-1/3}$, the same exponent that appears in eq. (11) and which is also compatible with ref. 22. The scaling for the flow velocity, eq. (12) has apparently never been observed before.

Past measurements of mass transport in finger convection²⁵⁻²⁸ have found good agreement between experimental data and a relation of the form $Sh \propto Ra_c^{1/3} f(Pr, Sc, \Lambda)$ with an undetermined function f , which is sometimes called the 4/3-law because this relation states that the mass flux varies as $\Delta c^{4/3}$ at constant Pr, Sc and Λ . Arguments in favor of this type of relation come from dimensional²⁵ and asymptotic analysis²¹. Eq. (13) can be rewritten as $Sh \propto Ra_c^{1/3} |\Lambda|^{-1/9} |Ra_T|^{1/36}$. The variation in $|Ra_T|^{1/36}$ is much too weak to be detectable in the experiment, so that eq. (13) must be considered to be indistinguishable from the 4/3-law.

IV. CONCLUSION

With an electrochemical technique, double diffusive convection can be investigated with a tabletop experiment for $Pr \approx 9$, $Sc \approx 2200$ and chemical Rayleigh numbers ranging from 5×10^8 to 10^{12} while varying the density ratio from 10^{-2} to 1. Fingers appear in all circumstances. The main quantities related to mass transport, the finger thickness, the flow velocity, and the concentration boundary layer thickness, are all independent of the cell height L , and depend on the concentration difference between top and bottom Δc as well as on the imposed temperature gradient $\Delta T/L$, but not on the temperature difference ΔT alone. The scaling for the Sherwood number proposed in eq. (13) is experimentally indistinguishable from the classical 4/3-law.

Perhaps the most remarkable finding is that fingers occur in the first place, considering the small stabilizing temperature gradient used here. It remains an open question whether there is an abrupt or a continuous transition from fingers to ordinary convection rolls which are at least as wide as they are tall. Eq. (11) remains correct down to the weakest stable stratification controllable in the experiment. In the case of a continuous transition, eq. (11) predicts that the small thermal Rayleigh number of $|Ra_T| \approx Ra_c^{1/3}$ is necessary for $d \approx L$.

This indicates that conditions suitable for finger formation are much more widespread than linear stability analysis suggests².

REFERENCES

- ¹J. Turner, “Multicomponent convection,” *Ann. Rev. Fluid Mech.*, **17**, 11–44 (1985).
- ²P. Baines and A. Gill, “On thermohaline convection with linear gradients,” *J. Fluid Mech.*, **37** (1969).
- ³M. Stern, “Collective instability of salt fingers,” *J. Fluid Mech.*, **35**, 209–218 (1969).
- ⁴W. Merryfield, “Origin of thermohaline staircases,” *Journal of Physical Oceanography*, **30**, 1046–1068 (2000).
- ⁵T. Radko, “What determines the thickness of layers in a thermohaline staircase?” *J. Fluid Mech.*, **523**, 79–98 (2005).
- ⁶K. Sreenivas, O. Singh, and J. Srinivasan, “On the relationship between finger width, velocity and fluxes in thermohaline convection,” *Phys. Fluids*, **21**, 026601 (2009).
- ⁷R. Krishnamurti, “Double-diffusive transport in laboratory thermohaline staircases,” *J. Fluid Mech.*, **483**, 287–314 (2003).
- ⁸R. Krishnamurti, “Heat, salt and momentum transfer in a laboratory thermohaline staircase,” *J. Fluid Mech.*, **638**, 491–506 (2009).
- ⁹C. Wagner, “The role of natural convection in electrolytic processes,” *J. Electrochem. Soc.*, **95**, 161–173 (1949).
- ¹⁰C. Wilke, M. Eisenberg, and C. Tobias, “Correlation of limiting currents under free convection conditions,” *J. Electrochem. Soc.*, **100**, 513–523 (1953).
- ¹¹Y. Kamotani, L. Wang, S. Ostrach, and H. Jiang, “Experimental study of natural convection in shallow enclosures with horizontal temperature and concentration gradients,” *Int. J. Heat Mass Transfer*, **28**, 165–173 (1985).
- ¹²W. Ward III and O. Le Blanc Jr., “Rayleigh-Bénard convection in an electrochemical redox cell,” *Science*, **225**, 1471–1473 (1984).
- ¹³R. Goldstein, H. Chiang, and D. See, “High-Rayleigh-number convection in a horizontal enclosure,” *J. Fluid Mech.*, **213**, 111–126 (1990).
- ¹⁴H. Chiang and R. Goldstein, “Application of the Electrochemical Mass Transfer Technique to the study of Bouyancy-driven Flows,” in *Transport Phenomena in Heat and Mass*

- Transfer* (Elsevier, Amsterdam, 1992) pp. 1–25.
- ¹⁵R. Probst, *Physicochemical Hydrodynamics* (John Wiley & Sons, New York, 1995).
- ¹⁶K.-Q. Xia, S. Lam, and S.-Q. Zhou, “Heat flux measurement in high-Prandtl-number turbulent Rayleigh-Bénard convection,” *Phys. Rev. Lett.*, **88**, 064501 (2002).
- ¹⁷G. Ahlers, S. Grossmann, and D. Lohse, “Heat transfer and large scale dynamics in turbulent Rayleigh-Bénard convection,” *Rev. Mod. Phys.*, **81**, 503–537 (2009).
- ¹⁸T. Hartlep, A. Tilgner, and F. H. Busse, “Large scale structures in Rayleigh-Bénard convection at high Rayleigh numbers,” *Phys. Rev. Lett.*, **91**, 064501 (2003).
- ¹⁹W. Malkus and G. Veronis, “Finite amplitude cellular convection,” *J. Fluid Mech.*, **4**, 225–260 (1958).
- ²⁰M. Proctor and J. Holyer, “Planform selection in salt fingers,” *J. Fluid Mech.*, **168**, 241–253 (1986).
- ²¹T. Radko and M. Stern, “Finite-amplitude salt fingers in a vertically bounded layer,” *J. Fluid Mech.*, **425**, 133–160 (2000).
- ²²T. Shirtcliffe and J. Turner, “Observations of the cell structure of salt fingers,” *J. Fluid Mech.*, **41**, 707–719 (1970).
- ²³T. Hosoyamada and H. Honji, “A thermohaline-diffusion tank with a movable plate,” *Experiments in Fluids*, **7** (1989).
- ²⁴P. Linden, “On the structure of salt fingers,” *Deep-Sea Research*, **20** (1973).
- ²⁵J. Turner, “Salt fingers across a density interface,” *Deep-Sea Res.*, **14**, 499–611 (1967).
- ²⁶R. Schmitt, “Flux measurements on salt fingers at an interface,” *J. Mar. Res.*, **37**, 419–436 (1979).
- ²⁷T. McDougall and J. Taylor, “Flux measurements across a finger interface at low values of the stability ratio,” *J. Mar. Res.*, **42**, 1–14 (1984).
- ²⁸J. Taylor and P. Bucens, “Laboratory experiments on the structure of salt fingers,” *Deep-Sea Research*, **36** (1989).